View metadata, citation and similar papers at core.ac.uk

brought to you by CORE

provided by Kyoto University Research Information Repository

KURENAI
Kyoto University Research Information Repository

KYOTO UNIVERSITY

Title	Latitudinal GRBR-TEC estimation in Southeast Asia region based on the two-station method
Author(s)	Watthanasangmechai, Kornyanat; Yamamoto, Mamoru; Saito, Akinori; Tsugawa, Takuya; Yokoyama, Tatsuhiro; Supnithi, Pornchai; Yatini, Clara Yono
Citation	Radio Science (2014), 49(10): 910-920
Issue Date	2014-10
URL	http://hdl.handle.net/2433/202824
Right	©2014. American Geophysical Union.; The full-text file will be made open to the public on 13 April 2015 in accordance with publisher's 'Terms and Conditions for Self-Archiving'.
Type	Journal Article
Textversion	publisher

Kyoto University

AGU PUBLICATIONS

Radio Science

RESEARCH ARTICLE
10.1002/2013RS005347

Key Points:
- Simple technique to estimate latitudinal GRBR-TEC in Southeast Asia
- Weighting function improves method's robustness during geomagnetic disturb
- GRBR-TEC can capture the EIA enhancements and the small-scale structure

Correspondence to:
K. Watthanasangmechai,
kukkai@rish.kyoto-u.ac.jp

Citation:
Watthanasangmechai, K., M. Yamamoto, A. Saito, T. Tsugawa, T. Yokoyama, P. Supnithi, and C. Y. Yatini (2014), Latitudinal GRBR-TEC estimation in Southeast Asia region based on the two-station method, *Radio Sci.*, *49*, 910–920, doi:10.1002/2013RS005347.

Received 22 NOV 2013
Accepted 19 SEP 2014
Accepted article online 23 SEP 2014
Published online 13 OCT 2014

Latitudinal GRBR-TEC estimation in Southeast Asia region based on the two-station method

Kornyanat Watthanasangmechai[1], Mamoru Yamamoto[1], Akinori Saito[2], Takuya Tsugawa[3], Tatsuhiro Yokoyama[3], Pornchai Supnithi[4], and Clara Yono Yatini[5]

[1]Research Institute for Sustainable Humanosphere (RISH), Kyoto University, Kyoto, Japan, [2]Department of Geophysics, Kyoto University, Kyoto, Japan, [3]National Institute of Information and Communications Technology, Tokyo, Japan, [4]King Mongkut's Institute of Technology Ladkrabang, Bangkok, Thailand, [5]National Institute of Aeronautics and Space of Indonesia, Indonesia

Abstract Total electron content (TEC) is an important parameter for revealing latitudinal ionospheric structures, such as the equatorial ionization anomaly (EIA) in Southeast Asia. Understanding the EIA is beneficial for studying equatorial spread *F*. To reveal the structures, the absolute TEC as a function of latitude must be accurately determined. In early 2012, we expanded a GNU Radio Beacon Receiver (GRBR) network to provide latitudinal coverage in the Thailand-Indonesia sector. We employed the GRBR network to receive VHF and UHF signals from polar low-Earth-orbit satellites. The TEC offset is an unknown parameter in the absolute TEC estimation process. We propose a new technique based on the two-station method to estimate the offset for the latitudinal TEC estimation, and it works better than the original method for a sparse network. The TEC estimation system requires two iterations to minimize the root-mean-square error (RMSE). Once the RMSE reaches the global minimum, the absolute TECs are estimated simultaneously over five GRBR stations. GPS-TECs from local stations are used as the initial guess of the offset estimation. The height of the ionospheric pierce point is determined from the ionosonde hmF2. As a result, the latitudinal GRBR-TEC was successfully estimated from the polar orbit satellites. The two EIA humps were clearly captured by the GRBR-TEC. The result was well verified with the TEC reconstructed from the C/NOFS density data and the ionosonde bottomside data. This is a significant step showing that the GRBR is a useful tool for the study of low-latitude ionospheric features.

1. Introduction

Southeast Asia is located in a low-latitude area covering both the northern and southern hemispheres. Above this region, the meridional total electron content (TEC) varies drastically as a function of time and position. The equatorial ionization anomaly (EIA) is one of the interesting phenomena in the low-latitude region, and it can be revealed by the variation in TEC. A recent method for measuring the TEC employs GPS networks to capture large-scale structures in the ionosphere [*Vladimer et al*., 1997; *Saito et al*., 1998; *Mendillo et al*., 2000; *Jiao et al*., 2013; *Emardson et al*., 2013; *Makarevich and Nicolls*, 2013]. A benefit of the GPS-TEC observation is that data are constantly available. In addition, the technique for the use of GPS to estimate the absolute TEC has been well studied [*Mannucci et al*., 1998; *Breed et al*., 1998; *Lunt et al*., 1999; *Makela et al*., 2001; *Otsuka et al*., 2002; *Ma and Maruyama*, 2003].

In addition to the GPS network, TEC observations are conducted by the differential Doppler measurement of dual-band beacon signals of 150/400 MHz from low Earth orbit (LEO) satellites. There are many studies that use this technique in midlatitude areas [*Evans et al*., 1983; *Leitinger et al*., 1984; *Ohta et al*., 1998]. Recently, networks of GNU Radio Beacon Receivers (GRBRs) were deployed in low-latitude regions to study longitudinal structures of the ionosphere by using the beacon signal from the Communication/Navigation Outage Forecasting System (C/NOFS) satellite [e.g., *Thampi et al*., 2009; *Tulasi Ram et al*., 2012].

To derive the absolute TEC from the differential Doppler measurement, however, the initial offset must be estimated. The offset must be determined at every satellite pass. The well-known two-station method was introduced by *Leitinger et al*. [1975]. This technique assumes that the absolute vertical TEC (V_a) measured from adjacent stations at the same ionospheric pierce point (IPP) in an overlapping region are the same, $V_{a1} = V_{a2}$. The method of least squares was used to solve for the unknown TEC offset. This two-station method has been widely used to estimate TEC offsets in dual-band beacon experiments for studies in the midlatitude

©2014. American Geophysical Union. All Rights Reserved.

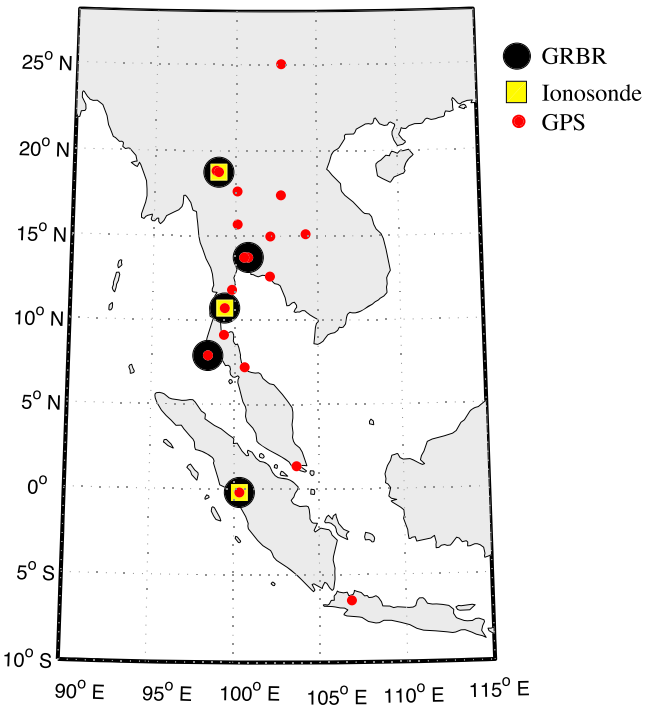

Figure 1. The distribution of the GNU Radio Beacon Receiver (GRBR), ionosonde, and GPS stations.

regions. But *Tulasi Ram et al.* [2012] reported a case that the two-station method failed when it was applied to the longitudinal TEC distribution in low-latitude regions. It is thus necessary to find an appropriate technique to estimate the absolute TEC in each situation.

In 2012, the GRBR network in Southeast Asia was extended in the meridional direction in the Thailand-Indonesia sector. It then became possible to study the meridional TEC distribution across the geomagnetic equator by receiving signals from polar orbit satellites. As the duration of a typical pass of a LEO satellite is about 20 min, we can estimate that the ionosphere does not change significantly during a single pass of the satellite. It is thus possible to detect the meridional distribution of TEC with higher temporal/spatial resolution than is possible with GPS-TEC observations. In this paper we introduce a new method for estimating the absolute TEC from our meridional chain of GRBRs.

The robustness of the two-station method largely depends on the configuration of the stations and the ionospheric conditions. Accuracy of the two-station method was demonstrated to be higher than that of the single-station method within a 5° longitudinal span between the stations [*Leitinger et al.*, 1975]. We first applied the classic two-station method to estimate our latitudinal GRBR-TEC in Southeast Asia. The GRBR network in Southeast Asia, however, is too sparse to allow the GRBR-TEC to be determined by this method. The method of least squares should minimize the discrepancy in the TEC estimates of adjacent stations. But in many cases, the fitting stopped at the local minimum; this was especially common when the signals were passing through a disturbed ionosphere. In other words, a simple least squares fitting was not sufficient to reach a global minimum of the discrepancy. Estimating the latitudinal GRBR-TEC from the sparse network is a challenge that has not yet been met. Therefore, as shown in this paper, we developed a new technique to derive the latitudinal distribution of the TEC using dual-band beacon signals for the low-latitude region.

2. Data

The ground-based data used in this work were obtained from five GRBRs, seventeen GPS receivers, and three ionosondes, all of which were located in Southeast Asia. The distribution of GRBR, GPS, and ionosonde stations is shown in Figure 1. In addition to the ground-based data, data from the C/NOFS satellite are used.

The five GRBR receivers were located at Kototabang (0.20°S, 100.32°E), Phuket (7.90°N, 98.39°E), Chumphon (10.72°N, 99.37°E), Bangkok (13.73°N, 100.78°E), and Chiang Mai (18.76°N, 98.93°E). Beacon signals from polar-orbiting LEO satellites were chosen because they provide wide latitudinal coverage. The polar-orbiting satellites used in this work include COSMOS2407, COSMOS2429, COSMOS2454, COSMOS2463, RADCAL, and DMSPF15. The orbits of these satellites are in the altitudinal range of 757 km to 1021 km. The seventeen GPS stations were distributed from 25°N to 10°S and from 98°E to 108°E. The three ionosondes were located at Kototabang (0.20°S, 100.32°E), Chumphon (10.72°N, 99.37°E), and Chiang Mai (18.76°N, 98.93°E).

To estimate the absolute GRBR-TEC, GPS-TEC was used as the first guess. The ionosonde hmF2 was used to decide the IPP height. The absolute GRBR-TEC was verified by the TEC generated from the ionosonde bottomside profile and C/NOFS data for the topside.

©2014. American Geophysical Union. All Rights Reserved.

3. Methodology

3.1. Estimation of the Absolute GRBR-TEC

To determine the latitudinal variation of the GRBR-TEC, we introduced a simple method that offsets the TEC measurement from the chain of GRBRs. GRBR observations provide only phase information, which allows precise TEC tracking. The GRBR-TEC is obtained from the phase difference (Φ) of the dual-frequency beacon signals, which operate at frequencies of 150 and 400 MHz. Normally, the 50 MHz frequency is used as the common frequency (f_r) for the beacon signals. The relation between the frequency and the ratio is as $f_1 = q_1 f_r$ and $f_2 = q_2 f_r$, where f_1 and f_2 are 150 and 400 MHz, respectively, and q_1 and q_2 are the ratios of the beacon frequencies to the common frequency. The phase difference Φ in radians at the common frequency (f_r) is expressed by the first term in the Taylor expansion of the true formula as

$$\Phi = \frac{\phi_2}{q_2} - \frac{\phi_1}{q_1} = \frac{\pi A}{f_r c}\left[\frac{1}{{q_2}^2} - \frac{1}{{q_1}^2}\right]\int N dx + \eta, \tag{1}$$

where ϕ_1 and ϕ_2 are the phases corresponding to $f_1 = 150$ MHz and $f_2 = 400$ MHz, respectively; $q_1 = 3$, $q_2 = 8$, $f_r = 50$ MHz for the beacon signals, $c = 2.998 \times 10^8$ m/s is the speed of light, $A = \frac{e^2}{(2\pi)^2 m \varepsilon_0} = 80.6\ \mathrm{m^3\ s^{-2}}$, $\varepsilon_0 = 8.854 \times 10^{-12}\ \mathrm{F\ m^{-1}}$ is the permittivity of free space, $e = -1.602 \times 10^{-19}$ C and $m = 9.109 \times 10^{-31}$ kg are the charge and mass of an electron, respectively; $\int N dx$ is the slant TEC along the radio wave path, and η is an unknown phase offset in radians [*Yamamoto*, 2008]. The TEC is usually described in TEC units (TECU), 1 TECU $= 1 \times 10^{16}$ electron/m^2.

The dual-band beacon experiment measures the slant TEC, which varies as a function of the satellite location and time. This is mainly due to changes in the elevation angle of the satellite and the spatial variation of the ionospheric plasma [*Yamamoto*, 2008]. Because of an unknown phase offset η in equation (1), the measured TEC is only the relative variation along a satellite-to-receiver path; the relative slant TEC (S_r); and

$$S_r = \Phi\left(\frac{\pi A}{f_r c}\left[\frac{1}{{q_2}^2} - \frac{1}{{q_1}^2}\right]\right)^{-1} = \int N dx + \eta', \tag{2}$$

where η' is the TEC offset, which is constant over one pass of a satellite at each station:

$$\eta' = \eta\left(\frac{\pi A}{f_r c}\left[\frac{1}{{q_2}^2} - \frac{1}{{q_1}^2}\right]\right)^{-1}. \tag{3}$$

With the assumption of a thin layer, estimation of the absolute TEC is discussed below. The absolute slant TEC (S_a) is then expressed as

$$S_a = \int N dx = S_r - \eta', \tag{4}$$

and the absolute vertical TEC (V_a) is expressed as

$$V_a = S_a \cos\chi, \tag{5}$$

where χ is the zenith angle of the satellite at the IPP. If we substitute equation (4) into equation (5), the absolute vertical TEC (V_a) can be derived from the relative slant TEC (S_r) as

$$V_a = (S_r - \eta')\cos\chi. \tag{6}$$

The satellite zenith angle at the height (h_i) of the IPP is given by

$$\chi = \sin^{-1}\left[\left(\frac{R_e}{R_e + h_i}\right)\cos\varepsilon\right], \tag{7}$$

where $R_e = 6{,}378.13 \times 10^3$ m is the mean radius of the Earth, ε is the elevation angle of the line of sight from the receiver to the satellite, and h_i is the height of the IPP. The relative vertical TEC (V_r) can be written as a function of the relative slant TEC (S_r) as

$$V_r = S_r \cos\chi, \tag{8}$$

equation (6) becomes

$$V_a = V_r - \eta'\cos\chi. \tag{9}$$

©2014. American Geophysical Union. All Rights Reserved.

Leitinger et al. [1975] proposed the two-station method to estimate TEC offsets that is widely known as a suitable technique for dual-band beacon experiments. The assumption is that the absolute vertical TECs derived from two stations at the same IPP in the region in which the adjacent station pairs overlapped will be the same if the stations are aligned along the same longitude (latitude); that is,

$$V_{a1} = V_{a2}. \tag{10}$$

The difference between V_{a1} and V_{a2} can be negligible if the zonal (meridional) TEC gradient is not too large when the assumption was applied on the low- (high-) inclination satellites. If we substitute equation (9) into equation (10), we obtain

$$V_{r1} - V_{r2} = \eta_1' \cos\chi_1 - \eta_2' \cos\chi_2. \tag{11}$$

For a number of IPP locations in the common region, the TEC offset (η') can be solved by the method of least squares.

When the two-station method was applied to the longitudinal distribution of the TEC, *Tulasi Ram et al.* [2012] showed that the method with the simple least squares approach failed to determine the TEC offsets. This was due to the longitudinal variation of the TEC with a spatial scale of several hundreds of km or less. The failure was primarily the result of the method of least squares, which overly adjusted the small-scale fluctuations of the TEC distribution.

Tulasi Ram et al. [2012] then introduced a single-station method with the assumption that the absolute vertical TEC (V_a) varies quasilinearly with horizontal distance, as expressed by

$$V_a = V_a^{\chi=\chi_c} + m \cdot x, \tag{12}$$

where χ is the satellite zenith angle, χ_c is the satellite zenith angle at the closest approach, m is the slope, and x lies in the eastward direction in a Cartesian coordinate system. If we substitute equation (12) into equation (9), we get

$$V_r = V_a^{\chi=\chi_c} + m \cdot x - \eta' \cos\chi, \tag{13}$$

where η' and m can be solved by nonlinear least squares fitting. This approach was successful for the longitudinal distribution of the TEC, as the model closely matched the situation.

As is generally known, the fountain effect generates the double hump of the equatorial anomaly. The single-station method designed for the longitudinal TEC distribution is not valid for the latitudinal TEC estimation because of this double hump. We thus introduce a new method for deriving the latitudinal GRBR-TEC over the equatorial region of Southeast Asia. The sparseness of the GRBR network breaches the assumption that was made when using the method of least squares with the two-station method. We propose a new way to determine the TEC offset by using widely distributed GRBR receivers and the absolute TEC data from local GPS receivers as follows: GPS-TEC is employed as the first guess for estimating the initial TEC offset (η') in the two-station method. The IPP height is decided by the ionosonde hmF2. The criteria for choosing the optimum estimated GRBR-TEC is the global minimum root-mean-square error (RMSE).

With the thin-layer assumption, *Leitinger et al.* [1975] recommended for midlatitudes a two-station method that used a single IPP height 50 km above the height (h_s) of the maximum electron density. *Ohta et al.* [1998] opposed the assumption of a fixed IPP height in their midlatitude experiments, and they mentioned that fixing the height at 400 km caused a discontinuous TEC. In addition, the degree of the discontinuity apparently changed with different values of h_s. Once h_s is determined as a function of latitude, the absolute TEC can be calculated [*Ohta et al.*, 1998]. In this work, the IPP height (h_i) of the thin layer is determined by the variable h_s, which is based on the actual height of the ionosonde hmF2 as a function of latitude, as given by

$$h_i(k) = h_s(k) + 50 \text{ km}, \tag{14}$$

where k denotes the latitude of the IPP. Since there are three ionosondes, the IPP is linearly interpolated to cover the latitude range of 20°S to 40°N. The electron density from the topside of the ionosphere contributes more to the TEC than that from the bottomside of the ionosphere, and this is why we specified the IPP height with an extra 50 km from the peak height. The number 50 km was selected from experiments.

©2014. American Geophysical Union. All Rights Reserved.

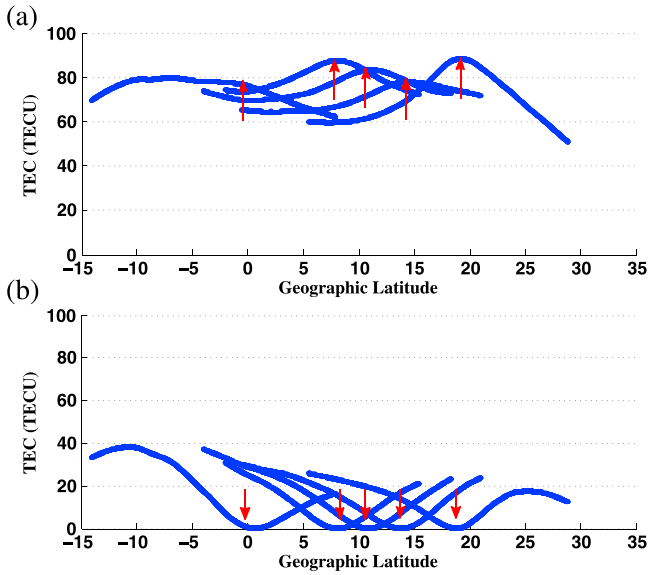

Figure 2. Examples of the effect of the initial total electron content (TEC) offset on the GRBR-TEC variation obtained from COSMOS2429 on 24 March 2012 from 10:31 UT (16:52 LT) to 10:46 UT (17:17 LT). (a) When the bias is too low, the shape of the GRBR-TEC is concave; (b) when it is too high, the shape is convex. Both cases are unrealistic. The arrows indicate the GRBR stations. The best fit was illustrated with the blue line in Figure 5a.

3.2. Estimation of the TEC Offset

Although derivation from the phase difference provides a precise variation in the TEC, the absolute TEC level is unknown, since the inherent TEC offset (η') is unknown. If the initial TEC offset (η') is too low, this causes the GRBR-TEC variation to be concave, while if it is too high, the variation is convex; this is shown in Figure 2. For multiple stations, the initial TEC offset (η') must be determined for each GRBR. At first, we tried to determine the TEC offsets from the GRBR network by fitting with the method of least squares applied to multiple stations. However, this did not work well in most cases because the system became stuck at a local minimum of the RMSE. We thus propose a method that finds the global minimum of the RMSE. The method is described below.

Step 1: Find the minimum RMSE by brute-force calculation of all possible TEC-offset combinations in a reasonable range based on the first guess by the GPS-TEC
Step 2: Sample the TECs at a resolution of 1° latitude; and
Step 3: Weight the RMSE such that the contributions from the edges of the data coverage are enhanced.

Step 1 is the key to finding the global minimum of the RMSE. Steps 2 and 3 are introduced to evaluate the RMSE over a wide latitudinal range. Step 2 helps to reduce the number of calculations, which is also achieved by the two-step (rough and precise) finding of the RMSE minimum, as shown below.

It is important to choose reasonable initial TEC offsets. We used the local GPS receiver network for this purpose. The GPS-TEC derived by the method reported by *Otsuka et al.* [2002] was used in forming the initial TEC-offset estimation. It does not directly affect the results of the GRBR-TEC.

Simultaneous determination of the five initial TEC offsets (η') for the five GRBR stations is possible if there are four overlapping regions. The GPS data that we used were as follows. The GPS-TEC data were selected at the IPP from the longitude range of 97.5°E to 102.5°E. The selected GPS-TEC data were divided into five groups. The center of each group was set at the latitude of a GRBR station, and the boundary was a distance of 5° latitude from the center. The mode value of each group was used as the first guess of the GRBR-TEC offset.

To select the optimum set of TEC offsets, we put all TEC offset candidates in a reasonable range to the test. Let S be the number of candidate TEC offsets in each set, and let N be the number of GRBR stations. Each absolute vertical TEC (V_a) combination was evaluated with a sampling interval of 1°. The intersect latitudes of each GRBR station were obtained. The RMSE of the overlapping GRBR-TECs for each of the S^N sets was calculated by

$$E = \sqrt{\sum_k \left[\sum_{i=1}^{N} \left[\sum_{J=1}^{N} \left(W_{ik} \cdot V_{a_{ik}} - W_{Jk} \cdot V_{a_{Jk}} \right)^2 \right] \right]}, \tag{15}$$

where E is the RMSE, i and j are the GRBR station numbers, k is the IPP latitude, N is the number of GRBR stations (here, $N = 5$), and V_a is the absolute vertical TEC. W is the weighting function that is defined by

$$W_k = \exp\left(\frac{|k - k_0|}{18} \right), \tag{16}$$

©2014. American Geophysical Union. All Rights Reserved.

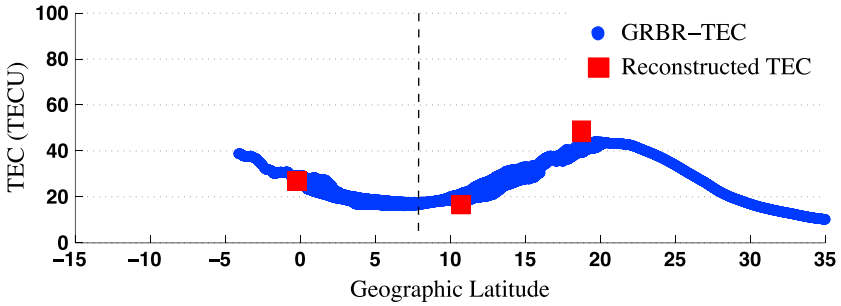

Figure 3. Comparison of the GRBR-TEC and the reconstructed TEC for 29 March 2012 between 13:12 UT (20:10 LT) and 13:33 UT (20:36 LT). The dashed vertical line indicates the dip equator latitude.

where W_k is the weight at a sampling point location, k is the IPP latitude in degrees, and k_0 is the latitude in degrees of the reference GRBR station. The number 18 is the number of half-latitudinal coverage in degrees for one satellite pass at the IPP altitude, for most cases.

The weight increased when the TEC was observed far from any of the GRBR locations. This means that there was more weight on the data at lower elevation angles. In the low-latitude region, the data availability was limited because a sharp EIA can cause the TEC to be overestimated at low angles of elevation. To avoid overestimating the TEC but still provide sufficient latitudinal coverage, the data with elevation angles less than 45° were excluded from the calculation of the RMSE.

The weighting and the data-selection criteria made it possible to find more reasonable TEC offsets during disturbed conditions of geomagnetically active periods. The selection of the weight function equation (16) was ad hoc, but the results very much improved the robustness of the TEC selection scheme. On the other hand, when the TEC distribution was smooth, the weighting did not affect the results.

For the first iteration, each TEC offset set spanned ±25 TECU around the first guess. Rough estimates of the offset candidates were selected at intervals of 5 TECU. There were 11 candidates for each GRBR station. We calculated the RMSE for all 11^5 possible combinations of the TEC offset and then selected those that yielded the minimum RMSE.

The second iteration more precisely estimated the TEC offset. The five TEC offset sets spanned ±3 TECU, centered around the five initial values that were obtained from the first iteration. The TEC offset candidates were selected at intervals of 1 TECU. Seven candidates were set for each GRBR station. We calculated the RMSE for all 7^5 combinations of offsets and determined which set yielded the minimum RMSE. This set of TEC offsets was used to estimate the absolute vertical TEC (V_a), also called the GRBR-TEC.

4. Validation of the Method

Figure 3 shows the latitudinal variations of the GRBR-TEC (the blue lines) on 29 March 2012 around 13:20 UT (20:20 LT). The GRBR-TEC was estimated with the COSMOS2407, which is the Russian LEO navigation satellite with a high-inclination orbit (83°). Its apogee and perigee are 1008 and 952 km, respectively. The COSMOS2407 was flying from north to south, and the ionospheric pierce point (IPP) of the GRBR-TEC variation distributed from 33.50°N, 104.60°E to 4.10°S, 105.80°E; between 13:12 UT (20:10 LT) and 13:33 UT (20:36 LT). This corresponds to 1.20° longitudinal separation of the IPP and 26 min LT coverage. There was a geomagnetic disturbance on 29 March 2012 ($K_p = 6$-). The solar activity was low on March 2012; the average number of sunspots was 65.

Figure 3 shows that the northern EIA crest appeared at 21.00°N, 105.07°E with 47.70 TECU. A local minimum of about 17 TECU appeared near 8°N, and this matches the geomagnetic equator. Unfortunately, the expected southern crest of the EIA could not be captured. This was due to a loss of lock near the end of the trajectory path at 4.12°S, 105.80°E. The GRBR network observed the latitudinal distribution of the TEC even under this disturbed condition. Small fluctuations were captured at both hemispheres between the dip equator and the EIA crests. There are several lines from different receivers overlapping in the figure. We calculated the standard deviation of the TECs in the overlapping regions. The average of all of the standard deviations was 1.74 TECU.

©2014. American Geophysical Union. All Rights Reserved.

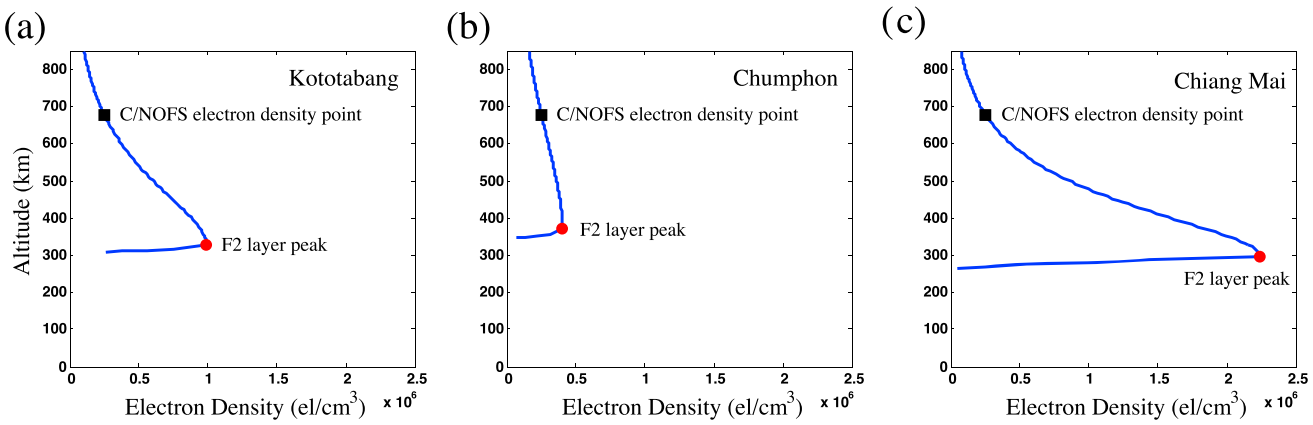

Figure 4. The vertical profiles of electron density, reconstructed from ionosonde and Communication/Navigation Outage Forecasting System (C/NOFS) density data at (a) Kototabang (0.20°S, 100.32°E), (b) Chumphon (10.72°N, 99.37°E), and (c) Chiang Mai (18.76°N, 98.93°E), for 29 March 2012 at 13:20 UT (20:20 LT).

The accuracy of the GRBR-TEC was examined by comparing it with the reconstructed TEC from the Southeast Asia Low-latitude Ionosonde Network (SEALION) [*Uemoto et al*., 2007] and density data from the C/NOFS satellite [*Stoneback et al*., 2013]. We traced the ionogram and converted the frequency height data to the real height profile of the plasma density by using the standard program, POLAN [*Titheridge*, 1979]. In order to calculate the TEC, we needed the density profile above the peak height of the ionosphere. We used the topside in situ ion density data measured by the C/NOFS Ion Velocity Meter (IVM), a part of the Couple Ion Neutral Dynamic Investigation (CINDI) [*Coley et al*., 2010]. The C/NOFS is a LEO satellite that is in a low-inclination orbit (13°) at an altitude between 375 and 710 km [*de La Beaujardière and the C/NOFS Science Definition Team*, 2004].

The method reported by *Tulasi Ram et al*. [2009] was used to reconstruct the TEC from the ionosonde and C/NOFS density data. The ionosonde was used to provide the bottomside density profile, while the C/NOFS in situ density data were used for the topside density profile. The scale height (H_T) between the ionospheric F2-layer peak and the C/NOFS height was determined. Using the same H_T with 1 km sampling, the vertical profile of the electron density was reconstructed between the lower boundary of the ionosphere and the C/NOFS height, and was extrapolated to higher altitudes.

The reconstructed vertical profiles of electron density at Kototabang (0.20°S, 100.32°E), Chumphon (10.72°N, 99.37°E), and Chiang Mai (18.76°N, 98.93°E) are shown in Figure 4. The topside data from the C/NOFS are also plotted in the figure. C/NOFS can provide in situ data at only a single location. For this calculation we selected the data at 13:20 UT (18:32 LT) at 2°N, 78°E and an altitude of 678 km. By using these profiles, we calculated the reconstructed TEC by integrating the electron density to the altitude of 1000 km. A small discrepancy between this height and the actual height of COSMOS2407 (952–1008 km) does not significantly change the reconstructed TEC. The results are indicated by red squares in Figure 3.

Differences between the GRBR-TEC and the reconstructed TEC were 1.44 TECU at Kototabang, 2.80 TECU at Chumphon, and 7.27 TECU at Chiang Mai. Considering the TEC estimate at each point, the discrepancy is 5.51% and 10.73% at Kototabang, and Chumphon, where the TEC from the GRBR network are in good agreement with the reconstructed TEC values. However, the discrepancy in the TEC estimates is largest (27.86%) over Chiang Mai. This might be attributable to the position of C/NOFS, which was orbiting near to Kototabang. The latitudinal distance between C/NOFS and Chiang Mai could be the reason for the discrepancy between the GRBR-TEC and the reconstructed TEC.

As seen in Figure 4, the ionosonde-reproduced bottomsides of the ionosphere are very steep, especially at Chiang Mai. The ionospheric bottom height in the geomagnetic southern hemisphere (Kototabang) was higher than that of the northern hemisphere (Chiang Mai). These features might be caused by a northward wind that diffuses the electrons along the field line to a lower altitude in the northern hemisphere. Even though a quantitative discussion is not yet possible, the in situ density data obtained in the southern hemisphere would be higher than the electron density at the same altitude in the northern hemisphere. This

©2014. American Geophysical Union. All Rights Reserved.

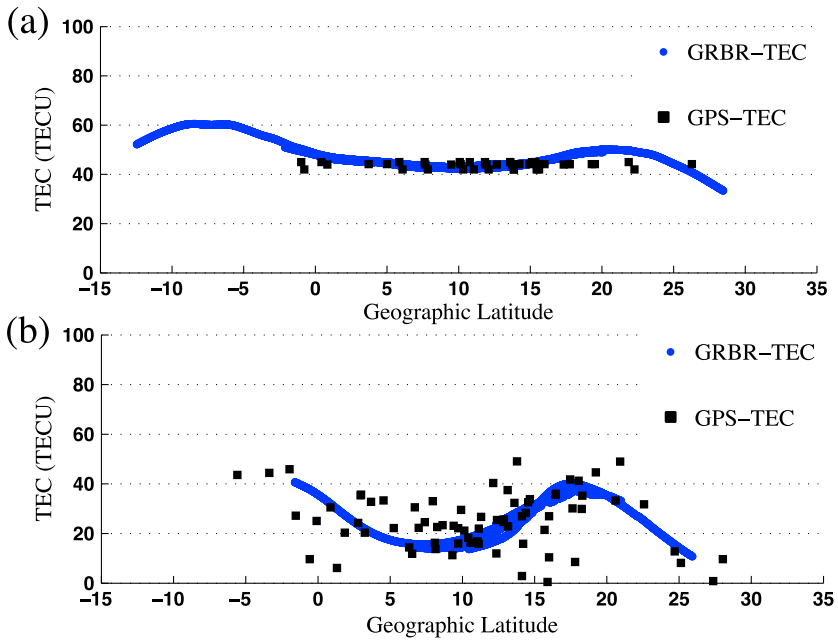

Figure 5. Comparison of the GRBR-TEC and GPS-TEC on 24 March 2012 (a) from 10:31 UT (16:52 LT) to 10:46 UT (17:17 LT), and (b) from 14:34 UT (21:10 LT) to 14:45 UT (21:25 LT).

overestimated topside electron density in the northern hemisphere might be the reason for the positive offset of the reconstructed TEC at Chiang Mai. Considering these factors, we can conclude that our technique produces a reasonable latitudinal distribution of the TEC, and estimating the TEC by a combination of polar-orbiting satellites and the GRBR network is successful.

5. Results and Discussions

The GRBR-TECs were produced on the day of the equinox, using data obtained from COSMOS2429 and COSMOS2407. The echoes received from the Equatorial Atmosphere Radar (EAR), which is located at 0.20°S, 100.32°E, were used to capture the equatorial spread *F* (ESF). On 24 March 2012, COSMOS2429 passed from 13.11°S, 95.55°E at 10:31 UT (16:52 LT) to 28.35°N, 97.73°E at 10:46 UT (17:17 LT), and COSMOS2407 passed from 25.78°N, 98.91°E at 14:34 UT (21:10 LT) to 1.99°S, 99.94°E at 14:45 UT (21:25 LT). The GRBR-TECs were estimated by the proposed method and are shown in Figure 5.

Figure 5a compares the GRBR-TEC and GPS-TEC, taken before sunset, from 10:31 UT (16:52 LT) to 10:46 UT (17:17 LT). This observation period is earlier than ESF occurrence. Neither the ESF nor the plasma bubble was seen. With the GRBR-TEC, we can clearly see two crests of the EIA enhancement with a 2° southward shift. This may be due to the meridional wind associated with the equatorial temperature and wind anomaly (ETWA) that is linked to the EIA [*Devasia et al*., 2002]. The northern EIA crest appeared at 23.00°N, 97.30°E with 45 TECU, while the southern EIA crest appeared at 9.00°S, 96.10°E with 62 TECU. The background GRBR-TEC is 45 TECU. The GRBR-TEC varies smoothly, with a RMSE of 0.50 TECU. The GPS-TEC also varies smoothly. In this case, the GPS-TEC shows similar value to the GRBR-TEC. GRBR-TEC is integrated plasma up to 1000 km, on average, while GPS-TEC is integrated plasma up to 22,000 km. GPS-TEC thus measures the plasmasphere in addition to the ionosphere. Considering this fact, the GPS-TEC should always be a few TECU more than GRBR-TEC. However, this feature is not seen in Figure 5a. The GPS-TEC would be underestimated by *Otsuka et al*. [2002] method when it is applied to low latitudes. From Figure 5a we should note that the latitudinal structure of the EIA is more clearly observed by the GRBR-TEC than by the GPS-TEC, despite the shallow peak in the northern hemisphere.

The variation of the GRBR-TEC at nighttime, from 14:34 UT (21:10 LT) to 14:45 UT (21:25 LT), is shown in Figure 5b. Taking into account the echoes from the EAR, as shown in Figure 6, we see that the ESF was active

©2014. American Geophysical Union. All Rights Reserved.

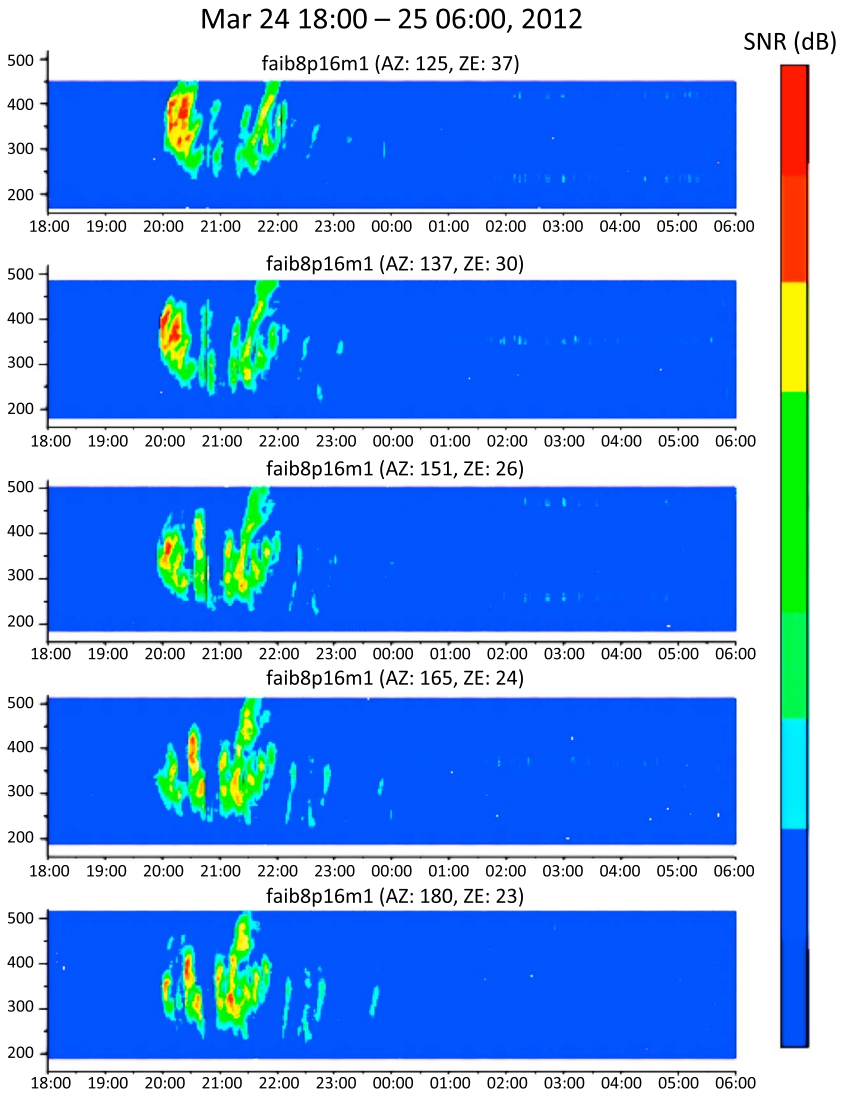

Figure 6. The Equatorial Atmosphere Radar (EAR) echoes on 24 March 2012. The plume appeared around 12:50 UT (19:50 LT) and lasted until local midnight.

when the COSMOS2407 flew over the GRBR station. The plume appeared around 12:50 UT (19:50 LT) and lasted until local midnight. As shown in Figure 5b, the GRBR-TEC was smoothly varying with some discrepancies between adjacent GRBR stations. The shallow ripples were seen in GRBR-TEC between 15°N and 20°N. It is the plasma bubble characteristic on the latitudinal GRBR-TEC. The field of view of the latitudinal GRBR observation is almost parallel to the plasma bubble structure that extends along the geomagnetic field. The structure seen in the GRBR-TEC is vague. When the shallow ripples are seen in the GRBR-TEC, the S4 index of the GRBR has a large value. This indicates the amplitude and phase scintillation of the GRBR due to the plasma bubble occurrence. The RMSE of the GRBR-TEC was 2.64 TECU, and the background GRBR-TEC was 28 TECU. The GRBR temporarily lost lock of the COSMOS2407 signal in the southern hemisphere on 24 March 2012 from 14:45 UT (21:25 LT) due to the scintillation. The GPS-TEC, on the other hand, shows scattering variation, which indicates the occurrence of a plasma bubble as well.

We note that the GRBR-TEC assumes a static ionosphere over the satellite pass (~20 min), while the GPS-TEC does not. The GRBR-TEC variation was reproduced from one satellite pass, while the GPS-TEC variation was reproduced by the combination of many satellites and receivers. Regarding the IPP, the GRBR has a longitudinal span of only 0.5° on average (see below), while the GPS data were selected from a 5° span

©2014. American Geophysical Union. All Rights Reserved.

around the GRBR sites. The scattered GPS-TEC reflects a large spatial variation in the TEC. The GRBR network, on the other hand, successfully measured the latitudinal structures of the ionosphere during the ESF event as having a longitudinal extent of the observation region that was smaller than that of the GPS-TEC.

With the EIA enhancement, the GRBR-TEC could capture only one crest due to its limited arc length. The arc-length shortening, which cannot be controlled, is caused by the lost-of-lock of the signals. It results in deficient overlapping latitudes. The captured northern crest located at 18.76°N, 99.46°E had 40 TECU. The south end of the GRBR-TEC variation, however, appears to be enhanced. We assume that this is part of another crest.

The most interesting physics occurs around the dusk terminator. For example, a zonal large-scale wave structure in the ionospheric electron content across the terminator was intensively studied by *Tulasi Ram et al*. [2012] and *Tulasi Ram et al*. [2014]. For the three cases discussed in this paper, as shown in Figures 3, 5a, and 5b, the zonal extent of their observation regions is discussed below.

The GRBR-TEC from the COSMOS2407 signals at local nighttime (20:10 LT – 20:36 LT) on 29 March 2012 are shown in Figure 3. The maximum zonal separation at the same latitude and the same IPP height was 1.20°. The average longitudinal separation was 0.50°. The average TEC discrepancy for a 1° longitudinal separation was 1.4 TECU. This discrepancy agrees with the results from *Tulasi Ram et al*. [2012]; in their Figure 3, the zonal variation of TEC at 20:18 LT was 1.3 TECU.

The GRBR-TEC from COSMOS2429 signals during the hour presunset (16:52 LT – 17:17 LT) on 24 March 2014 are illustrated in Figure 5a. The maximum zonal separation at the same latitude and the same IPP height was 1.90°. The average longitudinal separation was 0.70°. The average TEC discrepancy for a 1° longitudinal separation was 0.4 TECU. This discrepancy also agrees with the discussion by *Tulasi Ram et al*. [2012] that the zonal variation of the TEC is very small during the presunset period.

The GRBR-TEC from COSMOS2407 signals during a nighttime hour (21:10 LT – 21:25 LT) on 24 March 2014, when the ESF was active, are illustrated in Figure 5b. The maximum zonal separation at the same latitude and the same IPP height was 1.30°. The average longitudinal separation was 0.50°. The average TEC discrepancy for a 1° longitudinal separation was 1.5 TECU. This discrepancy agrees with the amplitude of the large-scale wave structure at night when the equatorial plasma bubbles were present, which is over 1 TECU in the Asian sector [*Tulasi Ram et al*., 2012].

From these cases, we find that the longitudinal fluctuation of the TEC is much smaller than the latitudinal TEC variability. The TEC data from the proposed technique are reasonable for all cases.

When the ESFs are present, the Earth's ionosphere is disturbed. This ionospheric disturbance introduced amplitude and phase uncertainties into the carrier signals used to measure the TEC. A quantitative estimate of the uncertainties is beyond the scope of this work. The effects from these uncertainties include fluctuations in the measured TEC [*McNamara et al*., 2013]. In this paper, the widest longitudinal separation at the IPP was 1.9° (211 km). The longitudinal scale size of the ESF is known to be several hundred kilometers [*Saito and Maruyama*, 2007]. The GRBR longitudinal separation and the ESF scale size are comparable. Although one example under such condition was successful, as shown in Figure 5b, we should be careful when applying the proposed technique to intense ESF events.

We analyzed additional data in March 2012. A preliminary discussion of the TEC estimation error is shown below. From 06:00 LT to 08:00 LT, before the EIA developed, all stations captured the TEC ripples with an error of 7% from the background TEC. The proposed method produced a GRBR-TEC with a 3% error from 09:00 LT to 17:00 LT. There was an unusual case on 8 March 2012 at 11:05 LT; the EIA crests were detected by the RADCAL satellite to be near the GRBR locations at Kototabang and Chiang Mai. The background TEC was higher than on other days at the same time, and this may indicate a strong day-to-day variability. The estimation error in this case was 8%. The best estimation had a 2% error and was obtained during the night and without the ESF from 18:00 LT to 20:00 LT. At night (18:00 LT – 20:00 LT) with the ESF, the error reached the maximum (10%). For the remainder of the night hours (21:00 LT – 02:00 LT), the estimation error was 3%. During 03:00 LT and 05:00 LT, the perturbations were seen from the GRBR chain, probably due to the post-midnight bubble or the dawn terminator. The error reached a maximum at 10%, which is the same level as that of the night with the ESF. It is beyond the scope of this paper to discuss in detail the physics of the ionosphere. More event studies will be presented in future works.

©2014. American Geophysical Union. All Rights Reserved.

6. Conclusions

Using the GPS-TEC as the first guess of the TEC offset values, we successfully estimated the biases for multiple GRBR stations. The proposed method finds the global minimum of the RMSE among all possible combinations of the TEC offset candidates. We used a two-step selection scheme to find the best combination of TEC offsets. Appropriate selection of the weighting function increases the robustness of the method. Results of the absolute TEC values were confirmed by comparison with the other TEC values from ionosondes and a C/NOFS satellite. It is obvious that the latitudinal TEC shows a double-hump distribution because of the equatorial anomaly. This is a promising method for studying the dynamics of the low-latitude ionosphere.

Acknowledgments

The authors acknowledge the support of the National Institute of Information and Communications Technology (NICT) for the ionosonde data from the SEALION project, and S. Saito for the ionogram tracking program. The C/NOFS (CINDI)-IVM data are provided through tthe University of Texas at Dallas supported by NASA grant NAS5-01068. This work was supported by JSPS KAKENHI grant 22403011 and 25302007, and MEXT Strategic Funds for the Promotion of Science and Technology. We thank R. Tsunoda and T. Maruyama for useful comments.

References

Breed, A. M., G. L. Goodwin, and J. H. Silby (1998), Total electron content measurements in the southern hemisphere using GPS satellites, 1991 to 1995, *Radio Sci.*, *33*(6), 1705–1726, doi:10.1029/98RS01856.

Coley, W. R., R. A. Heelis, B. J. Holt, and C. R. Lippincolt (2010), Ion temperature and density relationships measured by CINDI from the C/NOFS spacecraft during solar minimum, *J. Geophys. Res.*, *115*, A02313, doi:10.1029/2009JA014665.

de La Beaujardière, O., and the C/NOFS Science Definition Team (2004), C/NOFS: A mission to forecast scintillations, *J. Atmos. Sol. Terr. Phys.*, *66*, 1573–1591.

Devasia, C. V., N. Jyoti, K. S. Viswanathan, K. S. V. Subbarao, D. Tiwari, and R. Sridharan (2002), On the plausible linkage of thermospheric meridional winds with equatorial spread F, *J. Atmos. Sol. Terr. Phys.*, *64*, 1–12.

Emardson, R., P. Jarlemark, J. Johansson, and S. Schäfer (2013), Variability in the ionosphere measured with GNSS networks, *Radio Sci.*, *48*, 646–652, doi:10.1002/2013RS005152.

Evans, J. V., J. M. Holt, and R. H. Wand (1983), A differential-Doppler study of traveling ionospheric disturbances from Milstone Hill, *Radio Sci.*, *18*(3), 435–451, doi:10.1029/RS018i003p00435.

Jiao, Y., Y. T. Morton, S. Taylor, and W. Pelgrum (2013), Characteristic of high-latitude ionospheric scintillation of GPS signals, *Radio Sci.*, *48*, 698–708, doi:10.1002/2013RS005259.

Leitinger, R., G. Schmidt, and A. Tauriainen (1975), An evaluation method combining the differential Doppler measurement from two stations that enables the calculation of the electron content of the ionosphere, *J. Geophys.*, *41*, 201–213.

Leitinger, R., G. K. Hartmann, F.-J. Lohmar, and E. Putz (1984), Electron content measurements with geodetic Doppler receivers, *Radio Sci.*, *19*, 789–797, doi:10.1029/RS019i003p00789.

Lunt, N., L. Kersley, G. J. Bishop, A. J. Mazzella, and G. J. Bailey (1999), The effect of the protonosphere on the estimation of GPS total electron content: Validation using model simulations, *Radio Sci.*, *34*(5), 1261–1271, doi:10.1029/1999RS900043.

Ma, G., and T. Maruyama (2003), Derivation of TEC and estimation of instrumental biases from GEONET in Japan, *Ann. Geophys.*, *21*, 2083–2093.

Makarevich, R. A., and M. J. Nicolls (2013), Statistical comparison of TEC derived from GPS and ISR observations at high latitudes, *Radio Sci.*, *48*, 441–452, doi:10.1002/rds.20055.

Makela, J. J., M. C. Kelley, J. J. Sojka, X. Pi, and A. J. Mannucci (2001), GPS normalization and preliminary modeling results of total electron content during a midlatitude space weather event, *Radio Sci.*, *36*(2), 351–361, doi:10.1029/1999RS002427.

Mannucci, A. J., B. D. Wilson, D. N. Yuan, C. H. Ho, U. J. Lindqwister, and T. F. Runge (1998), A global mapping technique for GPS-derived ionospheric total electron content measurements, *Radio Sci.*, *33*(3), 565–582, doi:10.1029/97RS02707.

McNamara, L. F., R. G. Caton, R. T. Parris, T. R. Pederson, D. C. Thompson, K. C. Wiens, and K. M. Groves (2013), Signatures of equatorial plasma bubbles in VHF satellite scintillations and equatorial ionograms, *Radio Sci.*, *48*, 89–101, doi:10.1002/rds.20025.

Mendillo, M., B. Lin, and J. Aarons (2000), The application of GPS observations to equatorial aeronomy, *Radio Sci.*, *35*(3), 885–904, doi:10.1029/1999RS002208.

Ohta, Y., T. Maruyama, T. Okuzawa, K. Ohtaka, A. Morioka, and H. Kato (1998), Optimum mean ionospheric height in total electron content observations, *Proc. NIPR Symp. Upper Atmos. Phys.*, *11*, 121–130.

Otsuka, Y., T. Ogawa, A. Saito, T. Tsugawa, S. Fukao, and S. Miyazaki (2002), A new technique for mapping the total electron content using GPS network in Japan, *Earth Planets Space*, *54*, 63–70.

Saito, S., and T. Maruyama (2007), Large-scale longitudinal variation in ionospheric height and equatorial spread *F* occurrences observed by ionosondes, *Geophys. Res. Lett.*, *34*, L16109, doi:10.1029/2007GL030618.

Saito, A., S. Fukao, and S. Miyazaki (1998), High resolution mapping of TEC perturbations with the GSI GPS network over Japan, *Geophys. Res. Lett.*, *25*(16), 3079–3082, doi:10.1029/98GL52361.

Stoneback, R. A., R. A. Heelis, R. G. Caton, Y.-J. Su, and K. M. Groves (2013), In situ irregularity identification and scintillation estimation using wavelets and CINDI on C/NOFS, *Radio Sci.*, *48*, 388–395, doi:10.1002/rds.20050.

Thampi, S. V., M. Yamamoto, R. T. Tsunoda, Y. Otsuka, T. Tsugawa, J. Uemoto, and M. Ishii (2009), First observations of large-scale wave structure and equatorial spread F using CERTO radio beacon on the C/NOFS satellite, *Geophys. Res. Lett.*, *36*, L18111, doi:10.1029/2009GL039887.

Titheridge, J. E. (1979), Increased accuracy with simple methods of ionogram analysis, *J. Atmos. Sol. Terr. Phys.*, *41*, 243–350.

Tulasi Ram, S., S.-Y. Su, C. H. Liu, B. W. Reinisch, and L.-A. McKinnell (2009), Topside ionosphere effective heights (H_T) derived with ROCSAT-1 and ground-based ionosonde observations at equatorial and midlatitude stations, *J. Geophys. Res.*, *114*, A10309, doi:10.1029/2009JA014485.

Tulasi Ram, S., M. Yamamoto, R. T. Tsunoda, V. Thampi, and S. Gurubaran (2012), On the application of differential phase measurements to study the zonal large scale wave structure (LSWS) in the ionospheric electron content, *Radio Sci.*, *47*, RS2001, doi:10.1029/2011RS004870.

Tulasi Ram, S., M. Yamamoto, R. T. Tsunoda, H. D. Chau, T. L. Hoang, B. Damtie, M. Wassaie, C. Y. Yatini, T. Manik, and T. Tsugawa (2014), Characteristics of large-scale wave structure observed from African and Southeast Asia longitudinal sectors, *J. Geophys. Res. Space Physics*, *119*, 1–10, doi:10.1002/2013JA019712.

Uemoto, J., T. Ono, T. Maruyama, S. Saito, M. Lizima, and A. Kumamoto (2007), Magnetic conjugate observation of the F-3 layer using the SEALION ionosonde network, *Geophys. Res. Lett.*, *34*, L02110, doi:10.1029/2006GL028783.

Vladimer, J. A., M. C. Lee, P. H. Doherty, D. T. Decker, and D. N. Anderson (1997), Comparisons of TOPEX and global positioning system total electron content measurements at equatorial anomaly latitudes, *Radio Sci.*, *32*(6), 2209–2220, doi:10.1029/97RS02277.

Yamamoto, M. (2008), Digital beacon receiver for ionospheric TEC measurement developed with GNU Radio, *Earth Planets Space*, *60*, e21–e24.

©2014. American Geophysical Union. All Rights Reserved.